

## A NOTE ON THE CALCULATION OF CONSISTENT TANGENT OPERATORS FOR VON MISES AND DRUCKER–PRAGER PLASTICITY

RENÉ DE BORST

*Faculty of Civil Engineering, Delft University of Technology | Faculty of Mechanical Engineering, Eindhoven  
University of Technology*

AND

AREND E. GROEN

*Faculty of Civil Engineering, Delft University of Technology*

### SUMMARY

A comparison is made of implementations of consistent tangent operators that arise in implicit integration of Von Mises and Drucker–Prager yield criteria. When computing the consistent tangent operator a matrix inversion has to be performed at integration point level. The consequences of different formulations of the consistent tangent operator on the numerical accuracy are assessed.

### 1. INTRODUCTION

In recent years the concept of return-mapping algorithms has become popular for integrating differential stress–strain relations in plasticity. After application of the return-mapping scheme, a bijective relation has been established between the strain increment and the stress increment. When such a scheme is utilized in a Newton–Raphson strategy for achieving equilibrium at global level, this bijective relationship has to be differentiated in order to obtain the rate equations. Since a bijective relationship between stress and strain increments resembles the equations of a deformation plasticity theory, it is evident that a term arises during the differentiation process in which the plastic flow direction is differentiated with respect to the stress tensor. This observation has first been made by Simo and Taylor<sup>1</sup> and by Runesson *et al.*,<sup>2</sup> and the result is known as the consistent tangent operator.

During the construction of the consistent tangent operator a ‘modified elastic compliance’ matrix arises, which has to be inverted locally, i.e. in each integration point that is yielding. Principally, two different possibilities exist. Either the derivative of the flow direction with respect to the stress tensor is directly added to the elastic compliance matrix, or the compliance matrix is taken out of the brackets, so that the derivative of the plastic flow direction with respect to the stress tensor multiplied by the elastic stiffness matrix is added to the identity matrix. In either case this relation must be inverted to make the stress rate an explicit function of the strain rate, which is required for the tangent operator. Below we shall show that, depending on the value of Poisson’s ratio and the possible existence of singularities in the yield surface, large differences may arise during the numerical inversion of these matrices. This will be exemplified for the yield functions of Von Mises and Drucker–Prager.

## 2. MODEL FORMULATION

A first step in a return-mapping algorithm is the computation of a trial stress state

$$\boldsymbol{\sigma}^t = \boldsymbol{\sigma}^0 + \mathbf{D} \Delta \boldsymbol{\varepsilon} \quad (1)$$

with  $\boldsymbol{\sigma}^0$  the initial stress state,  $\mathbf{D}$  the elastic stiffness matrix and  $\Delta \boldsymbol{\varepsilon}$  the total strain increment. When the trial stress violates the condition that the yield function is non-positive,  $f(\boldsymbol{\sigma}^t, \kappa^0) \leq 0$ , with  $\kappa^0$  a scalar-valued hardening parameter evaluated at the beginning of the loading step, the trial stress is mapped onto the yield surface via the incremental version of the flow rule

$$\Delta \boldsymbol{\varepsilon}^p = \Delta \lambda \mathbf{m}(\boldsymbol{\sigma}^n) \quad (2)$$

with  $\boldsymbol{\varepsilon}^p$  the plastic strain tensor,  $\Delta \lambda$  the amount of plastic flow within this loading step and  $\mathbf{m}$  the flow direction. The fact that  $\mathbf{m}$  is determined for  $\boldsymbol{\sigma}^n$ , the stress at the end of the loading step, implies that a fully implicit scheme is utilized. In consideration of the additive split of the total strain increment into an elastic component  $\Delta \boldsymbol{\varepsilon}^e$  and a plastic component  $\Delta \boldsymbol{\varepsilon}^p$ , we obtain for the total incremental relation

$$\boldsymbol{\sigma}^n = \boldsymbol{\sigma}^0 + \mathbf{D} \Delta \boldsymbol{\varepsilon} - \Delta \lambda \mathbf{D} \mathbf{m}(\boldsymbol{\sigma}^n) \quad (3)$$

Differentiation of equation (3) leads to

$$\dot{\boldsymbol{\sigma}} = \mathbf{D} \dot{\boldsymbol{\varepsilon}} - \Delta \lambda \mathbf{D} \frac{\partial \mathbf{m}}{\partial \boldsymbol{\sigma}} \dot{\boldsymbol{\sigma}} - \dot{\lambda} \mathbf{D} \mathbf{m} \quad (4)$$

Defining the 'modified elastic compliance matrix' as

$$\mathbf{H} = \left[ \mathbf{D}^{-1} + \Delta \lambda \frac{\partial \mathbf{m}}{\partial \boldsymbol{\sigma}} \right]^{-1} \quad (5)$$

or equivalently

$$\mathbf{H} = \left[ \mathbf{I} + \Delta \lambda \mathbf{D} \frac{\partial \mathbf{m}}{\partial \boldsymbol{\sigma}} \right]^{-1} \mathbf{D} \quad (6)$$

equation (4) can be recast in the form

$$\dot{\boldsymbol{\sigma}} = \mathbf{H} \dot{\boldsymbol{\varepsilon}} - \dot{\lambda} \mathbf{H} \mathbf{m} \quad (7)$$

Formally, equations (5) and (6) are equal. However, during numerical inversion, differences can occur, as shown below.

Now consider the Drucker–Prager yield function

$$f = \sqrt{\left(\frac{3}{2} \boldsymbol{\sigma}^T \mathbf{P} \boldsymbol{\sigma}\right)} + \alpha \boldsymbol{\pi}^T \boldsymbol{\sigma} - k \quad (8)$$

with  $\alpha$  and  $k$  material parameters.  $\boldsymbol{\pi}$  is a vector that projects onto the hydrostatic axis in the stress space and  $\mathbf{P}$  is a projection matrix that projects a stress  $\boldsymbol{\sigma}$  onto the  $\pi$ -plane. Next we define  $\mathbf{m}$  as

$$\mathbf{m} = \frac{3 \mathbf{P} \boldsymbol{\sigma}}{2 \sqrt{\left(\frac{3}{2} \boldsymbol{\sigma}^T \mathbf{P} \boldsymbol{\sigma}\right)}} + \beta \boldsymbol{\pi} \quad (9)$$

which incorporates non-associated flow in case the dilatancy factor  $\beta$  differs from the friction factor  $\alpha$ . For this definition of the flow direction  $\mathbf{H}$  can be elaborated as

$$\mathbf{H} = \left[ \mathbf{D}^{-1} + \Delta \lambda \sqrt{\frac{3}{2}} \frac{\boldsymbol{\sigma}^T \mathbf{P} \boldsymbol{\sigma} \mathbf{P} - \mathbf{P} \boldsymbol{\sigma} \boldsymbol{\sigma}^T \mathbf{P}}{\boldsymbol{\sigma}^T \mathbf{P} \boldsymbol{\sigma} \sqrt{\left(\boldsymbol{\sigma}^T \mathbf{P} \boldsymbol{\sigma}\right)}}} \right]^{-1} \quad (10)$$

or

$$\mathbf{H} = \left[ \mathbf{I} + \Delta\lambda \sqrt{\frac{3}{2}} \mathbf{D} \frac{\boldsymbol{\sigma}^T \mathbf{P} \boldsymbol{\sigma} \mathbf{P} - \mathbf{P} \boldsymbol{\sigma} \boldsymbol{\sigma}^T \mathbf{P}}{\boldsymbol{\sigma}^T \mathbf{P} \boldsymbol{\sigma} \sqrt{(\boldsymbol{\sigma}^T \mathbf{P} \boldsymbol{\sigma})}} \right]^{-1} \mathbf{D} \quad (11)$$

respectively, depending on whether equation (5) or equation (6) is taken as the point of departure. It is noted that, because of non-commuting matrices, the expression between brackets in equation (11) becomes non-symmetric. However, symmetry is preserved for  $\mathbf{H}$ .

### 3. ACCURACY ANALYSIS

The accuracy of a matrix inversion can be characterized with the aid of the condition number. This quantity is defined by  $R = \lambda_n / \lambda_1$ , with  $\lambda_n$  the largest eigenvalue and  $\lambda_1$  the smallest eigenvalue of the matrix.<sup>3</sup> When the inverse of the condition number,  $R^{-1}$ , drops below the machine precision, matrix inversion is no longer possible.<sup>3</sup> For the less restrictive case that the inverse of the condition number,  $R^{-1}$ , is smaller than the square root of the machine precision, the matrix inversion is no longer reliable.<sup>3</sup>

Below we shall firstly assess the impact of the degree of elastic compressibility on  $R^{-1}$  for a stress point that is located on a smooth part of the Drucker-Prager yield surface, and then we shall investigate the case that it is near the apex of the yield cone. In both cases a Young's modulus  $E = 10^4$  MPa and a flow magnitude  $\Delta\lambda = 10^{-5}$  has been assumed. A threshold Jacobi method<sup>3</sup> has been used to extract the eigenvalues of  $\mathbf{H}$  set up for a plane-strain configuration. For the first case – the smooth part of the yield surface – the stress components have been assigned the values  $\sigma_1 = 1$  MPa,  $\sigma_2 = 1$  MPa,  $\sigma_3 = 0$ , so that  $\sqrt{(\frac{3}{2} \boldsymbol{\sigma}^T \mathbf{P} \boldsymbol{\sigma})} = 1$ . The inverse of the condition number,  $R^{-1}$ , been plotted in Figure 1 as a function of Poisson's ratio  $\nu$  for both formulations (5) and (6), or in this specific case for the Drucker-Prager yield function equations (10) and (11). We observe that, with increasing values of Poisson's ratio,  $R^{-1}$  deteriorates for formulation (10), but that it improves when equation (11) is used. For the case that the stress point is near the apex –  $\sigma_1 = 1$  MPa,  $\sigma_2 = 1$  MPa,  $\sigma_3 = 1 + 10^{-16}$  MPa, so that

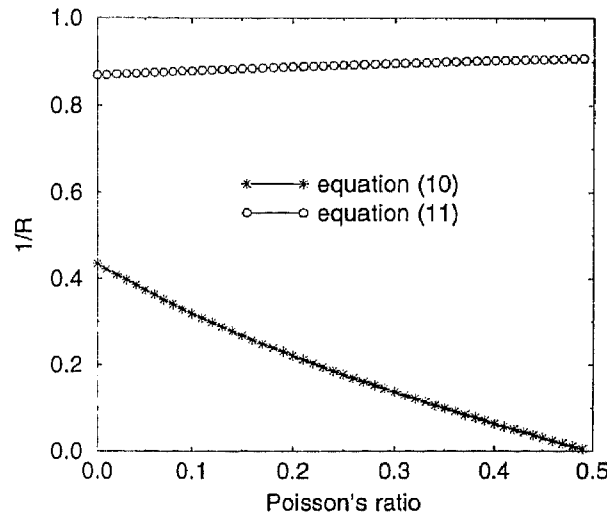


Figure 1.  $R^{-1}$  as a function of Poisson's ratio  $\nu$  for  $\sqrt{(\frac{3}{2} \boldsymbol{\sigma}^T \mathbf{P} \boldsymbol{\sigma})} = 1$  MPa

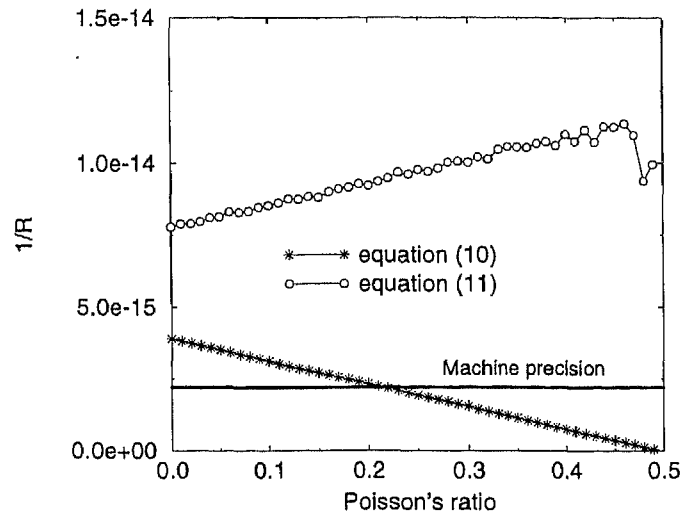


Figure 2.  $R^{-1}$  as a function of Poisson's ratio  $\nu$  for  $\sqrt{(\frac{3}{2}\sigma^T\mathbf{P}\sigma)} = 10^{-16}$  MPa

$\sqrt{(\frac{3}{2}\sigma^T\mathbf{P}\sigma)} = 10^{-16}$  – the difference between both formulations is even more pronounced, since the second term in equations (10) and (11) then becomes relatively more important with respect to the first term. The result of the eigenvalue analyses is summarized in Figure 2. As in the previous case the condition of (11) tends to improve when the incompressibility limit is approached, but again it becomes worse for equation (10). For  $\nu > 0.22$ ,  $R^{-1}$  even drops below the machine precision of the employed Silicon Graphics Indigo R4000 workstation, which implies that  $\mathbf{H}$  cannot be inverted.

The better condition of  $\mathbf{H}$  formulated according to equation (11) is due to the fact that the multiplication of  $\mathbf{D}$  with  $\partial\mathbf{m}/\partial\sigma$  eliminates the hydrostatic component of  $\mathbf{D}$ , or, equivalently, cancels the factor  $1 - 2\nu$  in the denominator of  $\mathbf{D}$ . This holds true for the Drucker–Prager and Von Mises yield criteria, and also for the Rankine yield function, since this criterion can also be cast in the format (8) with a flow direction vector according to (9), but with a different choice for  $\mathbf{P}$ .

#### 4. CONCLUDING REMARKS

Two different ways to implement the consistent tangent operator in elastoplasticity have been investigated with respect to their accuracy in cases of near-incompressible elasticity. It has been shown for the Drucker–Prager yield function that the formulation in which the elastic compliance matrix is taken out of the brackets prior to inversion is superior in the sense that it does not suffer from ill-conditioning of the local ‘modified elastic stiffness matrix’ when Poisson's ratio approaches a half. When the stress point is near the hydrostatic axis this ill-conditioning may even lead to an impossibility to invert the matrix, since the inverse of the condition number can become lower than the machine precision. Minor disadvantages of the more robust formulation are that locally non-symmetric matrices may arise and that an additional matrix multiplication is required.

## REFERENCES

1. J. C. Simo and R. L. Taylor, 'Consistent tangent operators for rate-independent elastoplasticity', *Comput. Methods Appl. Mech. Eng.*, **48**, 101–118 (1985).
2. K. Runesson, A. Samuelsson and L. Bernspang, 'Numerical technique in plasticity including solution advancement control', *Int. j. numer. methods eng.*, **22**, 769–788 (1986).
3. G. H. Golub and C. F. van Loan, *Matrix Computations*, The Johns Hopkins University Press, 1983.